

Free chlorine reactions of angiotensin II receptor antagonists: kinetics study, transformation products elucidation and in-silico ecotoxicity assessment

I. Carpinteiro, G. Castro, I. Rodríguez*, R. Cela

Department of Analytical Chemistry, Nutrition and Food Sciences. Institute for Research and Food Analysis (IIAA). Universidade of Santiago de Compostela, 15782 Santiago de Compostela, Spain.

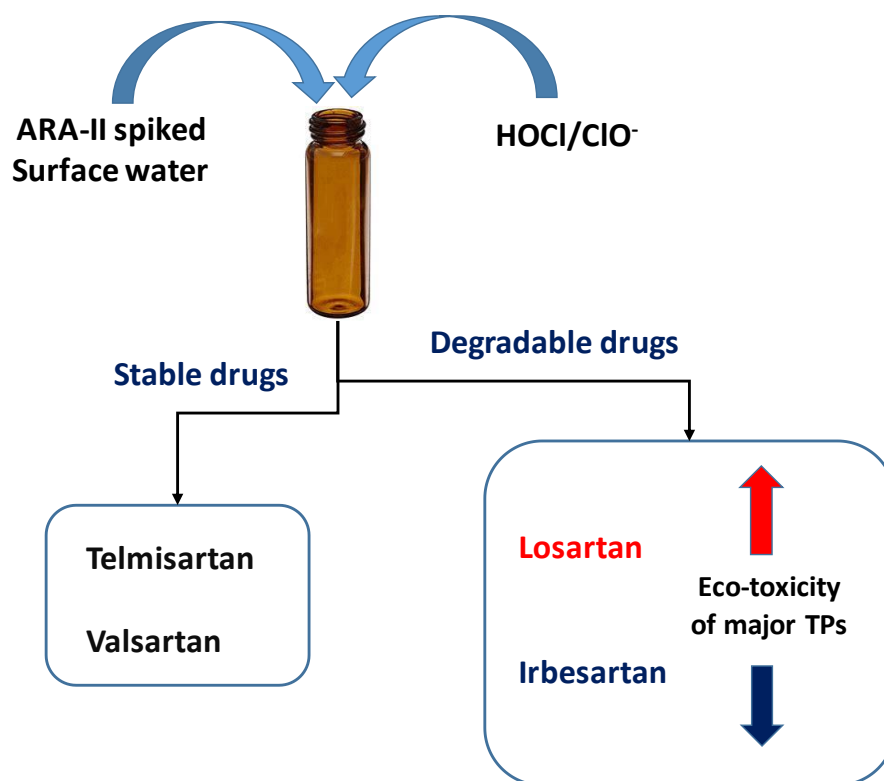
Publicado en:

Science of the Total Environment 647 (2019) 1000-1010

<https://doi.org/10.1016/j.scitotenv.2018.08.082>

Highlights:

- Sartans containing an imidazolic-like ring are degraded by free chlorine.
- Removal of reactive sartans fits a pseudo-first order kinetics model.
- Maximum degradation rates are observed at neutral, or slightly acidic, pHs.
- Imidazole halogenation represents the main reaction route of Losartan.
- Hydrolysis of the imidazolone ring explains most of the Irbesartan derivatives.



Graphical abstract

**Free chlorine reactions of angiotensin II receptor antagonists: kinetics study,
transformation products elucidation and in-silico ecotoxicity assessment**

I. Carpinteiro, G. Castro, I. Rodríguez*, R. Cela

Department of Analytical Chemistry, Nutrition and Food Sciences. Institute for Research and Food Analysis (IIAA). Universidade of Santiago de Compostela, 15782 Santiago de Compostela, Spain.

Abstract

Angiotensin II receptor antagonists (ARA II) are widely employed in the treatment of hypertension-related diseases. Because of their partial metabolization and limited biodegradability, these drugs have become ubiquitous pollutants in the aquatic environment, including surface water. This research evaluated the reactivity of the ARA II drugs: irbesartan (IRB), losartan (LOS) telmisartan (TEL) and valsartan (VAL) with free chlorine. Responses of parent compounds and their transformation products (TPs) were followed by liquid chromatography (LC) with quadrupole (Q) time-of-flight (TOF) mass spectrometry. Degradation experiments were carried out using ultrapure and river water samples, adjusted at different pHs and, in some cases, adding a small amount (ng mL^{-1} level) of bromide salts. Whilst TEL and VAL remained stable in presence of relatively high concentrations of free chlorine (10 mg L^{-1}), IRB and LOS were removed according to a pseudo-first order kinetics model. Considering an initial chlorine concentration of 10 mg L^{-1} , their half-lives varied between 6 and 734 min, depending mostly on the water pH. IRB reacted with free chlorine through hydroxylation processes, with and without molecular cleavage and re-arrangements in the imidazolone ring. Its TPs showed a lower *in-silico* predicted toxicity than the parent drug. In case of LOS, two major competitive degradation routes were identified. They involved replacement of the methanol group attached to the imidazole cycle by chlorine or bromine, and the cleavage of this cycle with removal of the chlorinated carbon and the nitrogen in alpha position. The TPs generated following the first route are predicted to be more toxic than LOS.

Keywords: Angiotensin II receptor antagonists; free chlorine; transformation products; liquid chromatography accurate mass spectrometry.

*corresponding author
e-mail: isaac.rodriquez@usc.es
Tel.0034881814387

1. Introduction

Angiotensin II receptor antagonists (ARA II) are a group of pharmaceuticals employed in the treatment of hypertension-related diseases. They are also termed under the generic name of sartans. The ageing and the lifestyle of occidental societies have led to a steady increase in the prescription of these drugs (Kasprzyk-Horden et al., 2009; Ortiz de García et al., 2013). Sartans are mostly excreted as parent compounds, with percentages of metabolization below 25% (Bayer et al., 2014). Consequently, they are present in urban sewage water at concentrations in the ng per mL⁻¹ range (Bodík et al., 2016; Oosterhuis et al., 2013; Stankiewicz et al., 2015). Their mass balances in conventional sewage treatment plants (STPs), equipped with primary and activated sludge units, showed variable, yet incomplete removal efficiencies. The levels of sartan drugs in the outlet streams of conventional STPs (equipped with primary and biological treatment units) represent between 20% and 80% of those found in influents (Gurke et al., 2015; Hermes et al., 2018; Kostich et al., 2014). Thus, sartans have also polluted the surface water compartment. In rivers impacted by the discharges of STPs, their concentrations stay in the range from 10 to 500 ng L⁻¹ (Giebułtowicz and Nałecz-Jawecki, 2016; Huerta-Fontela et al., 2011; Kasprzyk-Horden et al., 2008).

The stability of several ARA-II drugs, detected in polluted water resources, through the different stages involved in the production of drinking water has been previously reported (Giebułtowicz and Nałecz-Jawecki, 2016; Huerta-Fontela et al., 2011). Some data on the occurrence of sartans, and their primary biodegradation products at STPs (such as valsartan acid), in finished tap water have been also published (Giebułtowicz and Nałecz-Jawecki, 2016). However, no information is available neither regarding the variables affecting their half-lives ($t_{1/2}$) during chemical treatments of polluted waters (as those employed in the production of tap water), nor above the possible formation of transformation products (TPs) during these processes. To the best of our knowledge, the only TPs reported for sartan drugs correspond to those formed during biological treatment of urban wastewater (Letzel et al., 2015).

Free chlorine is one of the most popular oxidants during production of drinking water. Usually, pre-chlorination is the first step in the treatment of surface and/or groundwater resources. Free chlorine is also added to finished tap water in order to maintain its microbiological quality through the net of distribution pipes (Gibs et al., 2007; Postigo and Richardson 2014). Thus, residues of sartans existing in water catchments, and/or resisting to previous treatments (i.e. ozonisation, carbon filtration) applied during tap water production, might react with free chlorine leading to TPs with different chemical structures, and thus presenting different risks, than the parent pharmaceuticals, as it has been demonstrated for other emerging pollutants (Gibs et al., 2007; Temussi et al., 2013).

The aim of this research is to assess, for the first time, the behaviour of four sartans (irbesartan, IRB; losartan, LOS; telmisartan, TEL; and valsartan, VAL) during the treatment of surface water with free chlorine, at a laboratory scale. Except TEL, selected compounds present a biphenyl structure connected to a tetraazolic ring, which is considered as recalcitrant to biodegradation processes at STPs (Nödler et al., 2013). In Europe, VAL and IRB are the ARA II drugs with the highest consumption rates (Letzel et al., 2015); thus, they are susceptible to contaminate tap water sources. LOS was the first of the sartan drugs approved for the treatment of hypertension; nowadays, it is still prescribed for this purpose. Herein, the degradation rates of parent compounds, the identification and structural characterization of their TPs, and the *in-silico* estimation of their relative toxicities (versus those assigned to precursor molecules) are discussed. LC-QTOF MS is employed as analytical technique in the kinetics study and during elucidation of the structures of TPs. A preliminary evaluation of the TPs toxicities was obtained from quantitative structure-activity relationship (QSAR) data, using the ECOSAR, version 2.0, software package (<https://www.epa.gov/tsca-screening-tools/ecological-structure-activity-relationships-ecosar-predictive-model>).

2. Material and methods

2.1. Chemicals and samples

Standards of IRB, LOS (as potassium salt), TEL and VAL were obtained from Sigma-Aldrich (Milwaukee, WI, USA). Their chemical structures and some relevant physico-chemical properties are shown in Table 1. Positions in imidazolic cycles of IRB (imidazolone) and LOS (imidazole) are numbered, from 1 to 5 (see Table 1), to facilitate the discussion of their reactions with free chlorine. A standard of compound CAS number 748812-53-5, acquired from Sigma-Aldrich, was employed to discriminate between two possible structures compatible with the spectral data obtained for one of the TPs of IRB. Standards of each compound (600-1000 mg L⁻¹) were prepared in methanol, further dilutions and mixtures were made in the same solvent. The linear response range of the LC-QTOF MS system was evaluated with a second set of standards in ultrapure water.

Methanol (MeOH), HPLC-grade purity, sodium hydroxide and hydrochloric acid (37%) were purchased from Merck (Darmstadt, Germany). Ultrapure water (18.2 MΩ cm⁻¹) was obtained from a Milli-Q Gradient A-10 system (Millipore, Bedford, MA, USA). Potassium bromide, dipotassium hydrogen phosphate, potassium dihydrogen phosphate and ascorbic acid were supplied by Sigma- Aldrich (Steinheim, Germany). Solutions of the above salts were prepared in ultrapure water. Sodium hypochlorite (6-14% w/v) was acquired from Sigma-Aldrich. The exact concentration of this solution was determined by reaction with N,N-diethyl-p-phenylenediamine, with photometric detection (Clesceri et al., 1998), before being used in chlorination experiments.

River water, not affected by discharges from STPs, was obtained from a local stream. The sample was first filtered (using 0.45 μm filters) and then characterized in terms of carbon and inorganic species contents. The obtained values were: 1.4, 8.4, 8.4, 7.0 and 0.007 mg L⁻¹ of dissolved organic carbon, chloride, nitrate, sulfate and bromide ions, respectively. This matrix was used as representative of a catchment for drinking water production.

2.2. Chlorination experiments

The reactions between sartans and free chlorine were investigated in closed amber vials. A small volume (50-200 μL) of a methanolic standard of the considered compound was poured into the reaction vessel; then, 10 mL of water (ultrapure or the above described filtered river water) were added and the solution was homogenized in a vortex stirrer. Solutions were buffered at different pHs, in the range from pH 5 to 9 units, adding 1 mL of a 0.03 M solution of $\text{KH}_2\text{PO}_4/\text{K}_2\text{HPO}_4$. In some assays, potassium bromide was also introduced in the reaction vessel at levels from 0.067 to 0.30 mg L^{-1} (as bromide). Unless otherwise stated, the initial concentration of parent drugs was 0.250 mg L^{-1} (from 4.9 to 5.9 $\times 10^{-7}$ M, depending on their molecular weights). Free chlorine was added at concentrations of 2 or 10 mg L^{-1} (equivalent to 2.82 $\times 10^{-5}$ and 1.41 $\times 10^{-4}$ M, respectively), depending on the experiment. In both cases, a large molar excess of oxidant was employed. Thereafter, reaction vessels were capped, shaken for 2-3 s and left at room temperature (20 ± 2 $^\circ\text{C}$). Aliquots of 1 mL were collected at increasing times, from zero (before chlorine addition) to 1-48 h (depending on the rate of compounds degradation). Each reaction time aliquot was introduced in a 2 mL autosampler vial containing 0.01 mL of ascorbic acid (60 mg mL^{-1} solution in ultrapure water) to remove free chlorine and, thus, to stop any further oxidation reaction (Negreira et al., 2012). Vials were stored at 4 $^\circ\text{C}$ and injected in the LC-QTOF MS instrument, within the next 24 h.

A set of control experiments was performed with spiked water samples, buffered at different pHs (from 5 to 9 units), without chlorine addition. In this way, it was verified that sartans do not undergo other transformation reactions (e.g. hydrolysis), apart from those promoted by free chlorine. A second set of control assays was prepared in presence of chlorine, but without addition of sartans. Thus, false TPs, not correlated to parent compounds but arising from chlorine reaction with other organic species existing in river water, could be noticed.

2.3. Instrumentation

Parent compounds and their TPs were determined using a LC-QTOF MS instrument supplied by Agilent (Wilmington, DE, USA). The LC was an Agilent 1200 series consisting of a membrane degasser, two isocratic pumps, a chromatographic oven and an autosampler. The

QTOF mass spectrometer was an Agilent 6520 model, equipped with a dual electrospray ion source. Chromatographic separations were carried out in a Ultisil™ C₁₈ column (2.1 mm × 100 mm, 3 μm) provided by Welch Materials (Zhejiang, China). The analytical LC column was connected to C₁₈ guard cartridge (4 mm × 2 mm) supplied by Phenomenex (Torrance, CA, USA). Ultrapure water (A) and MeOH (B), both 0.1% in formic acid, were used as mobile phases. The LC gradient was programmed as follows: 0-0.5 min, 20% B; 15-17 min, 100% B; 18-29 min, 20% B. Column flow and temperature were set at 0.2 mL min⁻¹ and 30 °C, respectively. The injection volume of the different reaction time water aliquots was 30 μL.

Nitrogen (99.999%), used as nebulizing and drying gas in the electrospray ionisation source (ESI), was provided by a nitrogen generator (Erre Due srl, Livorno, Italy). Nitrogen (99.9995%) for collision-induced dissociation (MS/MS measurements) was purchased from Praxair (A Coruña, Spain). The ESI source was either operated in the (+) or (-) ionization modes, depending on the LC-QTOF MS experiment. The rest of ESI parameters were: drying gas temperature and flow-rate, 350 °C and 7 L min⁻¹, respectively; nebulizer gas pressure, 30 psi; capillary voltage, 4500 V; and fragmentor voltage, 150 V. The TOF instrument was operated at 2 GHz (extended-dynamic range mode) providing FWHM resolutions from 5000 (at *m/z* 121) to 10000 (at *m/z* 922 Da).

LC-QTOF MS control, data acquisition and processing were performed with the *MassHunter Workstation B.08.00* software (Agilent Technologies). The kinetics of chlorination reactions were followed in the ESI(+) mode, from responses obtained for the [M+H]⁺ ions of each parent drug (mass extraction window 10 ppm). The search of TPs was carried out in the LC-MS chromatograms acquired in both ionization modes (ESI+/-). MS spectra were recorded (at 2 spectra s⁻¹) in the range from 100 to 950 *m/z* units. LC-ESI MS records for control and different reaction time aliquots (n=3 replicates) were processed with the *MassHunter Profinder* software. This algorithm provides a list of molecular features with different intensities (potential TPs) in the above chromatograms. The empirical formula for each TPs was generated considering the accurate masses and the isotopic profiles for the clusters of ions in their ESI

(+)-MS and ESI (-) MS spectra. Normalized scores (1-100), accounting for mass accuracy and isotopic profile, are calculated from the fitting between the experimental spectra (in both ionization modes) and the expected (theoretical) ones for the empirical formula proposed for each TP. The ESI (+/-) MS/MS (product ion scan) spectra of each TP were acquired (4 spectra s^{-1}), in further LC runs, using different collision energies (5-40 eV). These spectra were interpreted for structural elucidation of the previously detected TPs.

2.4. In-silico ecotoxicity assessment

The ecotoxicity of parent sartans and their TPs to aquatic organisms were predicted using the ECOSAR software, freely available from the US Environmental Protection Agency (EPA). Predictions are based on the similarity of the investigated compound (parent drug or TP) to a set of chemicals, used to construct the QSAR model, whose environmental toxicities towards different organisms has been experimentally determined (Melnikow et al., 2016; Nika et al., 2017). In this work, 48-h *Daphnia magna* LC50 (50% lethal concentration), 96-h fish LC50 and 96-h green algae half-maximum effective concentration (EC50) were estimated. In addition, the chronic exposure toxicity values were obtained from the mean of non-observed effect concentration (NOEC) and the lowest observed effect concentration (LOEC), both predicted by ECOSAR software.

3. Results and discussion

3.1. Degradation kinetics

The linearity in the response of the LC-ESI(+) TOF MS system for parent drugs was investigated in the range of concentrations between 1 and 1000 $\mu\text{g L}^{-1}$. Within this interval, the plots of peak area versus concentration fitted a linear trend with determination coefficients (R^2) above 0.996. All compounds showed signal to noise ratios (S/N) above 10 for the lowest level standard solution. Thus, using 0.250 mg L^{-1} as their initial concentration in chlorination experiments, the potential degradation of sartans could be followed in an extent above 99%.

Preliminary degradation experiments were carried out with ultrapure water aliquots (pH 6.0), individually spiked with the investigated compounds, in presence of 10 mg L⁻¹ of free chlorine. Chlorine concentration and water pH can be considered as representative of those existing during pre-chlorination of raw water at drinking water production plants (Huerta-Fontela et al., 2011; Quintana et al., 2014). Solutions were allowed to react overnight (16 h), at room temperature. Thereafter, chlorine was removed and the response measured for each drug was compared with that obtained for the zero time aliquots. Chlorination assays and control experiments (without chlorine) were performed in triplicate. All compounds were stable in control samples. The concentrations of TEL and VAL remained also constant in the chlorinated water samples (non-significant variations after 16 h, n=3 replicates), whereas the levels of IRB and LOS were reduced around 90 and 95%, respectively. Fig. S1 shows the stability in the responses of TEL and VAL for reaction times between 2 and 16 h, in presence of 10 mg L⁻¹ of free chlorine. Thus, taking into account the relatively high concentration of chlorine, and the long reaction time employed in these previous experiments, only IRB and LOS are expected to undergo significant transformation reactions during free chlorine-based water disinfection treatments.

The effect of pH in the degradation rates of IRB and LOS was evaluated in the interval between 5 and 9 units. Assays were carried out in ultrapure water, using 10 mg L⁻¹ as the initial concentration of free chlorine. Reaction times aliquots were withdrawn at different times and the measured responses normalized to those observed at zero time. Then, the natural logarithmic of normalized values were plotted versus time. As compiled in the supplementary information (Table S1), the determination coefficients (R^2) of these graphs stayed above 0.990. Thus, within the investigated range of pH, the reactions of IRB and LOS with free chlorine followed pseudo-first order kinetics model. The values for their reaction rate constants (k , M⁻¹ min⁻¹), and the $t_{1/2}$ data are also included in Table S1.

Fig. 1 illustrates the dependence between the obtained $t_{1/2}$ data and the water pH. The $t_{1/2}$ values of LOS increased slightly from pH 5 to 7. Above pH 7, the stability of this drug increased

dramatically. In case of IRB, the measured $t_{1/2}$ increased smoothly when the pH of the water sample differed from 7. At basic pHs, the acid-base equilibrium of HOCl (pKa 7.58) is shifted towards the hypochlorite anion, which is less reactive than the acid form. At pH 5 the imidazolic-like sub-structure existing in the molecules of IRB and LOS is partially protonated, Table 1. In case of IRB the protonated imidazolone ring is believed to be less reactive than the neutral form. This hypothesis will explain the decrease of the $t_{1/2}$ of this sartan between pH 5 and 7. For LOS, the equilibrium between protonated and neutral forms of the imidazole ring did not affect its reactivity with free chlorine. Thus, the lower the sample pH the higher the concentration of HOCl, consequently the degradation of LOS was faster.

In addition to pH, the kinetics of reactions with free chlorine may be affected by organic and inorganic species existing in surface water. To investigate these effects, $t_{1/2}$ values were also calculated adding a small concentration of bromide (0.067 mg L^{-1} and 0.1 mg L^{-1} for ultrapure and river water, respectively) to samples. Experiments were performed at pH 7, using chlorine concentrations of 2 and 10 mg L^{-1} for IRB and LOS, respectively. Table 2 shows the obtained data. The degradation rate of IRB remained unaffected by the addition of bromide traces to both water matrices; however, the $t_{1/2}$ values in river water were twice longer than in ultrapure water. Regarding LOS, without bromide addition, similar $t_{1/2}$ were observed for ultrapure and river water. Addition of potassium bromide speed up the removal of LOS in both matrices, Table 2. Usually, bromide traces increase the rate of the reactions with free chlorine when parent compounds undergo halogenation processes (Quintana et al., 2014). In summary, the effects of pH, bromide and water matrix in the half-lives of IRB and LOS (Fig. 1 and Table 2, respectively) indicate that, although both drugs contain similar functionalities in their chemical structures (Table 1), they probably react with free chlorine following different routes.

3.2. Identification and characterization of TPs.

Table 3 summarizes the TPs detected in chlorination experiments. The list of compounds is limited to those displaying responses above 0.5% of that measured for the precursor drug (initial concentration 1 mg L⁻¹) at zero time. TPs are labelled according to the discussion of their chemical structures in further paragraphs. In addition to retention times and empirical formulae, the number of double bond equivalents (DBEs) and the normalized scores (values from 0-100, calculated as described in section 2.3), corresponding to the cluster of ions in their ESI (+) and ESI (-) MS spectra, are included in Table 3. Same data are also provided for the precursor drugs.

TPs arising from IRB incorporated extra atoms of oxygen, maintaining the same number of carbons. LOS led to halogenated (LOS-TPs 1 and 2), molecular cleavage (LOS-TPs 3 and 4) and a hydroxylated derivative (LOS-TP5). Compounds compiled in Table 3 were noticed in chlorination experiments with ultrapure and river water. The exception was IRB-TP4, which was found only in the ultrapure water chlorination assays. It is worth noting that, the brominated derivative of LOS (LOS-TP2) was formed even without increasing the level of bromide (0.007 mg L⁻¹) existing in the employed river water matrix. The structures of TPs compiled in Table 3 are discussed on the basis of fragment ions, observed in their ESI(+) and ESI(-) MS/MS spectra, recorded at different collision energies in the range from 5 to 40 eV. The most probable formula of each fragment was proposed with the aid of the *MassHunter* software, considering the elemental composition of the precursor ([M+H]⁺ or [M-H]⁻) ion.

Irbesartan

IRB-TP1 is a hydroxylated compound with the same DBE number as IRB, Table 3. Their ESI(+) product ion spectra contain a common fragment at *m/z* 207 Da (nominal value), which was assigned to the tetraazolic biphenyl moiety (C₁₄H₁₁N₄⁺) after losing two atoms of nitrogen (C₁₄H₁₁N₂⁺), Fig. 2A and 2B. The product ion at *m/z* 195.1489 u in the spectrum of IRB, which has been assigned to the imidazolone ring, appears at 211.1430 u in case of IRB-TP1. Thus,

hydroxylation necessarily occurred in any of the butyl chains (the linear or the cyclic one) connected to the imidazolone sub-structure. This assumption is confirmed with fragments in their ESI(-) MS/MS spectra provided as supplementary material (Fig. S2). Unfortunately, the ESI(+/-) MS/MS spectra of this TP did not contain enough information to establish which of the alkyl carbons was hydroxylated. IRB-TP1 was tentatively assigned to IRB hydroxylated in the terminal carbon of the linear butyl chain. This compound has been previously proposed as one of the TPs formed during the biodegradation of IRB in laboratory scale STPs (Letzel et al., 2015).

The spectra of IRB-TP2 are shown in Fig. 3. Fragments at m/z 252, 235 and 207 Da (nominal values) in the ESI(+) product ion spectrum (Fig. 3A) suggest hydroxylation of IRB followed by cleavage of one of the bonds with nitrogen 1 in the imidazolone cycle, Table 1. The two possible products of this reaction are a carboxylic acid or an amide, depending on whether hydroxylation takes place in carbon 5, or in carbon 2, of IRB, respectively. The carboxylic acid has been reported as a biodegradation product of IRB at STPs (Letzel et al., 2015), whilst the amide is known to be an impurity formed during the synthesis of IRB (Chando et al., 1997). Structures assigned to the rest of product ions in the ESI(+) spectrum of IRB-TP2 are compatible with both species. When examining the ESI(-) spectrum of the same TP (Fig. 3B), the product ion at 305.1650 u (assigned to fragment ion $C_{20}H_{21}N_2O$), and other fragment ions at lower m/z values (i.e. those at 211.1445 and 100.0768 u) point out to the amide structure. Final confirmation of the identity of IRB-TP2 was obtained by injection of a commercial standard of the amide derivative (CAS number 748812-53-5). Thus, IRB-TP2 is the result of hydroxylation of the imine carbon (carbon 2 in the imidazolone cycle of IRB, Table 1), followed by cleavage of the single bond between carbon 2 and nitrogen number 1 in the same cycle.

IRB-TPs 3 and 4 present the same empirical formula and DBE number as IRB-TP1; however, their spectra contain different fragments. The ESI (+) MS/MS spectrum of IRB-TP3 (Fig. 4A) shares some common ions with that of IRB-TP2 (Fig. 3A), such as those at 252 and 235 Da. Other ions differ in 2 Da (fragments at 194 and 166 Da for IRB-TP3, versus 196 and 168 for

IRB-TP2). A structure compatible with the spectrum in Fig. 4A corresponds to intramolecular cyclization between the hydroxylated terminal carbon of IRB-TP1 and carbon number 2 in the imidazolone cycle (Table 1), with further opening of this ring.

The ESI(+) MS/MS spectrum of IRB-TP4 (Fig.4B) contains fragments at higher m/z ratios than those observed for above described TPs. The product ion at m/z 250.1084 u (experimental value) suggest a similar structure to that of IRB-TP2 (Fig. 3A), but with an additional double bond. Likely, this unsaturation is located between the carbon in alpha to the biphenyl ring and the atom of nitrogen. The product ions at m/z 361.1743 and 316.1536 u (experimental values) are compatible with the above assumption. From these ions a second fragmentation route, which is common to most TPs of IRB, consists of the loss of two atoms of nitrogen from the tetraazolic ring to produce the major fragments at 333.1704 and 288.1485 u. The ion at m/z 195.0912 u is generated from removal of HCN from that at m/z 222.1015 u. The structure assigned to IRB-TP4 (Fig. 4B) is also compatible with the ESI(-) MS/MS spectrum of this compound (see supplementary information, Fig. S3).

The ESI(+) MS/MS spectrum of IRB-TP5 (Fig. 5) is very similar to that of IRB-TP3. The most significant differences are the fragments at m/z values of 210 and 182 Da in the spectrum of IRB-TP5 (Fig. 5) versus those at 194 and 166 obtained for the IRB-TP3 (Fig. 4A). IRB-TP5 is proposed to be generated from hydroxylation of IRB-TP3. Probably, hydroxylation takes place again in the imine carbon of TP3, evolving into a second amide functionality and a terminal carbonyl group to generate IRB-TP5 (Fig. 5). The oxidation of an imine moiety to produce an amide has been recently reported during the aqueous photodegradation of the neonicotinoid nitenpyram (González-Mariño et al., 2018). This oxidation reaction explains also the formation of IRB-TP2, whose identity has been confirmed using an authentic standard.

Losartan

LOS-TP1 and TP2 are di-halogenated species, Table 3. They are formed through replacement of the methanol group, attached to the imidazole cycle of LOS (Table 1), by chlorine (TP1) or

bromine (TP2). Likely, the reaction is initiated with an electrophilic attack to carbon number 5 in this ring, Table 1. Electrophilic halogenation is recognized as one of the most common reactions of aromatic pollutants with free chlorine (Nika et al., 2017; Negreira et al., 2012). The ESI(-) MS/MS spectra (Fig. S4) of both compounds contain an intense cluster of ions (191.0144 and 234.9635 u for LOS-TP1 and LOS-TP2, respectively) which correspond to the di-halogenated imidazole cycle linked to the butyl chain. The analogue fragment in the spectrum of LOS appears at m/z 187.0629 u, Fig. S4.

The MS/MS spectra for LOS-TP3, together with the assigned structure, is shown in Fig. 6. This TP is a non-halogenated species, containing two additional atoms of oxygen and losing CCIN in comparison to LOS, Table 3. Its ESI(+) MS/MS spectrum indicates that the biphenyl group attached to the tetraazolic ring has not undergone any modification (product ions at 235.0972 and 207.0906 u, Fig. 6A). The other intense ion in this spectrum appears at m/z 310.1277 u. Formation of LOS-TP3 involves hydroxylation of carbons number 2 and 5 in the imidazole ring of LOS (Table 1), followed by further oxidation to the corresponding carbonyl moieties with removal of CCIN. The ESI(-) MS/MS spectrum (Fig. 6B) is compatible with the structure proposed for this compound. Particularly, the ions at 308, 252 and 158 Da (nominal masses) contain valuable information regarding the chains attached to the tertiary atom of nitrogen in the molecule of LOS-TP3.

LOS-TP4 is likely a secondary TP of LOS. It is generated from the loss of the two carbons chain bonded to tertiary nitrogen in LOS-TP3. The fragment at m/z 100.0769 u in the ESI(-) MS/MS spectrum of the TP (Fig. S5) confirms the existence of a butyl amide group in the structure of this species. Finally, LOS-TP5 is a hydroxylated derivative of LOS. The very weak signal obtained for this compound prevented obtaining its product ion spectrum; so, the exact hydroxylation position could not be investigated.

3.3. TPs stability and transformation routes

The time-course of the TPs described in the previous section was followed in samples buffered at pH 7, considering reaction times up to 8 h. Fig. 7 shows the profiles obtained for river water

aliquots, previously spiked with IRB and LOS, in presence of 2 and 10 mg L⁻¹ of free chlorine, respectively. Bromide was not added to the river water aliquots in these experiments. Values in the Y axis are normalized responses (ratios between the peak areas of each compound and that for the precursor at zero time, multiplied by 100) represented versus reaction time. In the particular case of IRB-TP2, the molar yield of its formation has been calculated and plotted versus the reaction time.

As shown in Fig. 7A, the response of IRB-TP2 reached a maximum after 2 h and then, it remained practically unchanged. This species is the major TP formed in the reaction of IRB with free chlorine. Additional chlorination experiments using water samples spiked with this TP demonstrated its negligible degradation after 8 h (less than 5% and 6% in river and ultrapure water, respectively) in presence of 10 mg L⁻¹ of chlorine. Responses for IRB-TPs 1 and 3 remained practically stable after 1 h. Their maximum normalized values represented around 1% of the IRB response at zero time; thus, they are considered minor TPs. On the other hand, the signal of IRB-TP5 increased continuously within the considered reaction time (Fig. 7A), which supports the idea of being a secondary TP or IRB.

The levels of the halogenated derivatives of LOS (LOS-TPs 1 and 2) reached a maximum after 4 h, whilst the responses obtained for LOS-TPs 3 and 4 rose steadily within the considered reaction time (Fig. 7B). The response of the hydroxylated derivative (LOS-TP5) stayed at very low levels: around 0.2%. Under experimental conditions considered in Fig. 7 (river water containing 0.007 mg L⁻¹ of bromide in presence of 10 mg L⁻¹ of free chlorine), the dichlorinated species (LOS-TP1) was the TP formed in a higher extent; however, in bromide richer samples, the ratio between the responses for the dichloro (LOS-TP1) and the bromochloro (LOS-TP2) derivatives might differ. Such situation is depicted in the supplementary information section with the time-course plots of both TPs in river water aliquots spiked with increased concentrations of bromide, Fig. S6.

Taking into account the structures assigned to identified TPs and their time-course during chlorination assays, the possible reaction routes of sartans with chlorine are proposed, Fig. 8.

IRB-TP2 is the major TP of IRB. It is formed through hydroxylation of the imine double bond, with opening of the imidazolone ring. TPs 1, 3 and 4 are generated following competitive hydroxylation routes. Structure assigned to IRB-TP1 remains as tentative. IRB-TP5 is a secondary TP arising from IRB-TP3. For LOS, electrophilic substitution halogenation appears to be the most important of the identified reaction routes. A competitive transformation path involves hydroxylation with cleavage of the imidazole ring, followed by further N-dealkylation.

3.4. Toxicity assessment

A key issue when oxidative treatments lead to formation of organic derivatives from known emerging pollutants is to predict whether the new compounds represent an environmental hazard, or not. In this vein, it is convenient to compare the acute and the chronic toxicities of the precursor molecules and those corresponding to the identified TPs. *In-silico* models provide preliminary data to answer the above question with a minimum cost. The LC-50 concentrations for acute and chronic exposure to the investigated compounds, considering three different model organisms, are given as supplementary material, Table S2. The ratios between their relative LC-50 values (TP/parent drug) are compiled in Table 4. Values below the unit correspond to enhanced estimated toxicities, whereas, values above 1 point out to a reduced toxicity. The reaction of IRB with free chlorine led to a lower predicted toxicity. However, the di-halogenated derivatives of LOS (LOS-TPs 1 and 2), and the secondary derivative (LOS-TP4) showed ratios below 1; whereas, that of LOS-TP3 remains around the unit. Thus, the interaction of LOS with free chlorine might lead to an enhancement in the toxicity of the solution.

4. Conclusions

The imidazolic-like rings of IRB (imidazolone cycle) and LOS (imidazole cycle) are responsible for their reactivity with free chlorine. On the other hand, the benzoimidazole and the tetraazolic biphenyl cycles in the structures of the investigated drugs did not interact with oxidant. Thus,

TEL and VAL will remain unchanged during free chlorine treatments employed in the production of tap water, whilst IRB and LOS disappear following pseudo-first order kinetics, with maximum reaction rates at neutral, or slightly acidic pHs.

IRB interacts with free chlorine through different hydroxylation and oxidation reactions. The most favourable one involves carbon number 2 in the imidazolone cycle, followed by ring opening and oxidation of the imine to an amide. LOS mostly undergoes electrophilic substitution of methanol by one halogen (chlorine or bromine) in position 5 of the imidazole ring. This reaction path competes with cleavage of the same ring, concurrently to double hydroxylation and loss of CCIN. *In-silico* predictions point out to a decrease of the toxicity during IRB reactions with free chlorine; however, the opposite effect is expected for LOS.

Acknowledgements

This study was supported by Xunta de Galicia (grant GRC-ED431C 2017/36), and the Spanish Government (grant CTQ2015-68660-P). I.C. acknowledges a postdoctoral fellowship to Xunta de Galicia.

Declarations of interest: none.

References

Bayer, A., Asner, R., Schüssler, W., Kopf, W., Weiß, K., Sengl, M., Letzel, M., 2014. Behavior of sartans (antihypertensive drugs) in wastewater treatment plants, their occurrence and risk for the aquatic environment. *Environ. Sci. Pollut. Res.* 21, 10830–10839. <https://doi.org/10.1007/s11356-014-3060-z>.

Bodík, I., Mackuľak, T., Fáberová, M., Ivanová, L., 2016. Occurrence of illicit drugs and selected pharmaceuticals in Slovak municipal wastewater. *Environ. Sci. Pollut. Res.* 23, 21098–21105. <https://doi.org/10.1007/s11356-016-7415-5>.

Chando, T.J., Everett, D.W., Kahle, A.D., Starret, A.M., Vachharajani, N., Shyu, W.C., Kripalani, K.J., Barbhैया, R.H., 1997. Biotransformation of irbesartan in man. *Drug Metab. Dispos.* 26, 408-417.

Clesceri, L.S., Greenberg, A.E., Eaton, A.D. (Eds.), 1998. *Standard Methods for the Examination of Water and Wastewater*, 20th ed., American Water Works Association, Baltimore, MD.

Ecological Structure Activity Relationship, <https://www.epa.gov/tsca-screening-tools/ecological-structure-activity-relationships-ecosar-predictive-model>, v 2.0, accessed June 2018.

Gibs, J., Stackelberg, P.E., Furlong, E.T., Meyer, M., Zaugg, S.D., Lippincott, R.L., 2007. Persistence of pharmaceuticals and other organic compounds in chlorinated drinking water as a function of time. *Sci. Total Environ.* 373, 240–249. <https://doi.org/10.1016/j.scitotenv.2006.11.003>.

Giebuľtowicz, J., Nałecz-Jawecki, G., 2016. Occurrence of cardiovascular drugs in the sewage-impacted Vistula River and in tap water in the Warsaw region (Poland), *Env. Sci. Pollut. Res.* 23, 24337–24349. <https://doi.org/10.1007/s11356-016-7668-z>.

González-Mariño, I., Rodríguez, I., Rojo, L., Cela, R., 2018. Photodegradation of nitenpyram under UV and solar radiation: Kinetics, transformation products identification and toxicity prediction. *Sci. Total Environ.* 644, 995-1005. <https://doi.org/10.1016/j.scitotenv.2018.06.318>.

Gurke, R., RoBler, M., Marx, C., Diamond, S., Schubert, S., Oertel, R., Fauler, J., 2015. Occurrence and removal of frequently prescribed pharmaceuticals and corresponding metabolites in wastewater of a sewage treatment plant. *Sci. Total Environ.* 532, 762–770. <https://doi.org/10.1016/j.scitotenv.2015.06.067>.

Hermes, N., Jewell, K.S., Wick, A., Ternes, T.A., 2018. Quantification of more than 150 micropollutants including transformation products in aqueous samples by liquid chromatography-tandem mass spectrometry using scheduled multiple reaction monitoring. *J. Chromatogr. A.* 1531, 64–73. <https://doi.org/10.1016/j.chroma.2017.11.020>.

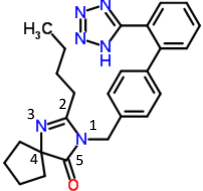
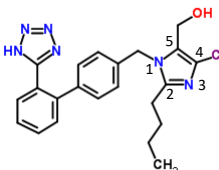
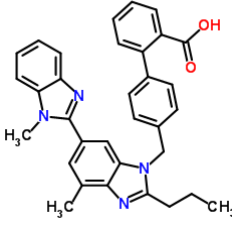
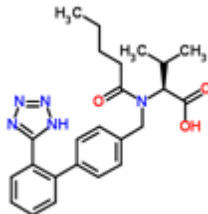
Huerta-Fontela, M., Galceran, M.T., Ventura, F., 2011. Occurrence and removal of pharmaceuticals and hormones through drinking water treatment. *Water Res.* 45, 1432–1442. <https://doi.org/10.1016/j.watres.2010.10.036>.

Kasprzyk-Hordern, B., Dinsdale, R.M., Guwy, A.J., 2008. The occurrence of pharmaceuticals, personal care products, endocrine disruptors and illicit drugs in surface water in South Wales, UK. *Water Res.* 42, 3498–3518. <https://doi.org/10.1016/j.watres.2008.04.026>.

- Kasprzyk-Hordern, B., Dinsdale, R.M., Guwy, A.J., 2009. Illicit drugs and pharmaceuticals in the environment - Forensic applications of environmental data. Part 1: Estimation of the usage of drugs in local communities. *Environ. Pollut.* 157, 1773–1777. <https://doi.org/10.1016/j.envpol.2009.03.017>.
- Kostich, M.S., Batt, A.L., Lazorchak, J.M., 2014. Concentrations of prioritized pharmaceuticals in effluents from 50 large wastewater treatment plants in the US and implications for risk estimation. *Environ. Pollut.* 184, 354–359. <https://doi.org/10.1016/j.envpol.2013.09.013>.
- Letzel, T., Bayer, A., Schulz, W., Heermann, A., Lucke, T., Greco, G., Grosse, S., Schüssler, W., Sengl, M., Letzel, M., 2015. LC-MS screening techniques for wastewater analysis and analytical data handling strategies: Sartans and their transformation products as an example. *Chemosphere* 137, 198–206. <https://doi.org/10.1016/j.chemosphere.2015.06.083>.
- Melnikow, F., Kostal, J., Voutchkova-Kostal, A., Zimmerman, J.B., Anastas, P.T., 2016. Assessment of predictive models for estimating the acute aquatic toxicity of organic chemicals. *Green Chem.* 18, 4432–4445. <https://doi.org/10.1039/C6GC00720A>.
- Negreira, N., Rodríguez, I., Rodil, R., Cela, R., 2012. Assessment of benzophenone-4 reactivity with free chlorine by liquid chromatography time-of-flight mass spectrometry. *Anal. Chim. Acta* 743, 101–110. <https://doi.org/10.1016/j.aca.2012.07.016>.
- Nika, M.C., Bletsou, A.A., Koumaki, E., Noutsopoulos, C., Mamis, D., Stasinakis, A.S., Thomaidis, N.S., 2017. Chlorination of benzothiazoles and benzotriazoles and transformation products identification by LC-HR-MS/MS. <https://doi.org/10.1016/j.jhazmat.2016.03.035>.
- Nödler, K., Hillebrand, O., Idzik, K., Strathmann, M., Schipperski, F., Zirlewagen, J., Licha, T., 2013. Occurrence and fate of the angiotensin II receptor antagonist transformation product valsartan acid in the water cycle - A comparative study with selected β -blockers and the persistent anthropogenic wastewater indicators carbamazepine and acesulfame. *Water Res.* 47, 6650–6659. <https://doi.org/10.1016/j.watres.2013.08.034>.
- Oosterhuis, M., Sacher, F., ter Laak, T.L., 2013. Prediction of concentration levels of metformin and other high consumption pharmaceuticals in wastewater and regional surface water based on sales data. *Sci. Total Environ.* 442, 380–388. <https://doi.org/10.1016/j.scitotenv.2012.10.046>.
- Ortiz de García, S., Pinto Pinto, G., García Encina, P., Irusta Mata, R., 2013. Consumption and occurrence of pharmaceutical and personal care products in the aquatic environment in Spain. *Sci. Total Environ.* 444, 451–465. <https://doi.org/10.1016/j.scitotenv.2012.11.057>.
- Postigo, C., Richardson, S.D., 2014. Transformation of pharmaceuticals during oxidation / disinfection processes in drinking water treatment. *J. Hazard. Mater.* 279, 461–475. <https://doi.org/10.1016/j.jhazmat.2014.07.029>.
- Quintana, J.B., Rodil, R., Rodríguez, I., 2014. Transformation Products of Emerging Contaminants upon Reaction with Conventional Water Disinfection Oxidants. In: Nollet, L., Lambropoulou, D. (Eds.), *Transformation Products of Emerging Contaminants in the Environment*. Wiley, Chichester, pp. 123–160. <https://doi.org/10.1002/9781118339558.ch04>.
- Stankiewicz, A., Giebułtowicz, J., Stankiewicz, U., Wroczyński, P., Nałecz-Jawecki, G., 2015. Determination of selected cardiovascular active compounds in environmental aquatic samples - Methods and results, a review of global publications from the last 10 years. *Chemosphere* 138, 642–656. <https://doi.org/10.1016/j.chemosphere.2015.07.056>.

Temussi, F., DellaGreca, M., Pistillo, P., Previtera, L., Zarrelli, A., Criscuolo, E., Lavorgna, M., Russo, C., Isidori, M., 2013. Sildenafil and tadalafil in simulated chlorination conditions: Ecotoxicity of drugs and their derivatives. *Sci. Total Environ.* 463-464, 366–373. <https://doi.org/10.1016/j.scitotenv.2013.05.081>.

Table 1. Chemical structures, CAS number, log D values (pH7) and pK_a values of sartan compounds considered in the study.

Name	Abbreviation	CAS number	Structure	Log D (pH 7) ^a	pK _a ^a
Irbesartan	IRB	138402-11-6		3.36	4.29 ^b 4.08 ^c
Losartan	LOS	114798-26-4		2.84	4.26 ^b 3.82 ^c
Telmisartan	TEL	144701-48-4		5.17	3.62 ^b 4.57 ^c 5.86 ^c
Valsartan	VAL	137862-53-4		0.43	4.00 ^b 4.61 ^b

^aCalculated values obtained with the ChemAxon software

^bAcidic group

^cBasic group

Table 2. Half-lives ($t_{1/2}$, min, with their errors) measured in water samples buffered at pH 7. Initial concentration of free chlorine 2 and 10 mg L⁻¹ for IRB and LOS, respectively.

Compound	Ultrapure water		^b River water	
	Without bromide	^a 0.067 mg L ⁻¹ bromide	No bromide addition	^a 0.100 mg L ⁻¹ bromide
IRB	21.8 ± 0.8	22.0 ± 0.7	40 ± 2	40 ± 1
LOS	39.5 ± 0.8	26.0 ± 0.7	39.8 ± 0.8	21 ± 1

^a Added bromide concentration.

^b The river water matrix contained 0.007 mg L⁻¹ of bromide.

Table 3. Summary of transformation products (TPs) observed during chlorination experiments in water samples spiked with IRB and LOS.

Compound	Retention time (min)	Empirical formula	DBEs	Score [M+H] ⁺	Score [M-H] ⁻	^a Exact mass
IRB	16.30	C ₂₅ H ₂₈ N ₆ O	15	99.52	99.24	428.2333
IRB-TP1	14.86	C ₂₅ H ₂₈ N ₆ O ₂	15	99.60	80.44	444.2272
IRB-TP2	16.61	C ₂₅ H ₃₀ N ₆ O ₂	14	98.36	99.33	446.2443
IRB-TP3	16.17	C ₂₅ H ₂₈ N ₆ O ₂	15	99.45	98.50	444.2272
IRB-TP4	18.13	C ₂₅ H ₂₈ N ₆ O ₂	15	95.11	83.25	444.2272
IRB-TP5	15.00	C ₂₅ H ₂₈ N ₆ O ₃	15	83.20	76.38	460.2225
LOS	16.87	C ₂₂ H ₂₃ ClN ₆ O	14	99.59	97.32	422.1622
LOS-TP1	18.35	C ₂₁ H ₂₀ Cl ₂ N ₆	14	99.04	99.25	426.1123
LOS-TP2	18.31	C ₂₁ H ₂₀ ClBrN ₆	14	99.67	98.54	470.0621
LOS-TP3	16.54	C ₂₁ H ₂₃ N ₅ O ₃	13	99.61	99.78	393.1800
LOS-TP4	15.95	C ₁₉ H ₂₁ N ₅ O	12	90.77	97.69	335.1746
LOS-TP5	15.88	C ₂₂ H ₂₃ ClN ₆ O ₂	14	84.49	97.77	438.1571

^aMonoisotopic exact mass for the neutral species.

Table 4. Ratios between estimated toxicities (TP/precursor drug) for the TPs of IRB and LOS under acute and chronic exposure. Values obtained from the ECOSAR software toxicity predictions.

TP	Acute toxicity			Chronic toxicity		
	Fish	Daphnid	Algae	Fish	Daphnid	Algae
	LC ₅₀ (96h)	LC ₅₀ (48h)	EC ₅₀ (96h)	LC ₅₀ (96h)	LC ₅₀ (48h)	EC ₅₀ (96h)
IRB-TP1	33	44	16	13	23	7
IRB-TP2	121	180	46	34	72	15
IRB-TP3	5.9	6.8	4.2	3.5	5.0	2.7
IRB-TP4	67	94	28	22	43	10
IRB-TP5	221	367	287	760	6.7	37
LOS-TP1	0.03	0.12	0.20	0.19	0.11	0.21
LOS-TP2	0.02	0.09	0.17	0.17	0.09	0.19
LOS-TP3	1.1	1.3	n.a.	0.95	8	n.a.
LOS-TP4	0.0005	0.008	0.025	0.275	0.008	n.a.

n.a.: not available data.

Captions to figures.

Fig. 1. Effect of pH in the half-lives ($t_{1/2}$ min) of IRB and LOS. Data for ultrapure water solutions using 10 mg L^{-1} of free chlorine, without bromide addition.

Fig. 2. ESI (+) MS/MS spectra for IRB (A) and IRB-TP1 (B).

Fig. 3. Proposed structure and ESI (+) (A) and ESI (-) (B) product ion spectra for IRB-TP2.

Fig. 4. ESI (+) MS/MS spectra of IRB-TP3 (A) and IRB-TP4 (B).

Fig. 5. Structure and ESI (+) MS/MS spectra of IRB-TP5.

Fig. 6. Chemical structure and ESI (+) (A) and ESI (-) (B) product ion scan spectra for LOS-TP3.

Fig. 7. Time-course of TPs identified in the chlorination experiments using river water aliquots. A, data for IRB in presence of 2 mg L^{-1} of chlorine. B, data for LOS using 10 mg L^{-1} of chlorine.

Fig. 8. Proposed reaction pathways for IRB (A) and LOS (B) in chlorinated water samples. Tentatively identified compounds are marked with an asterisk.

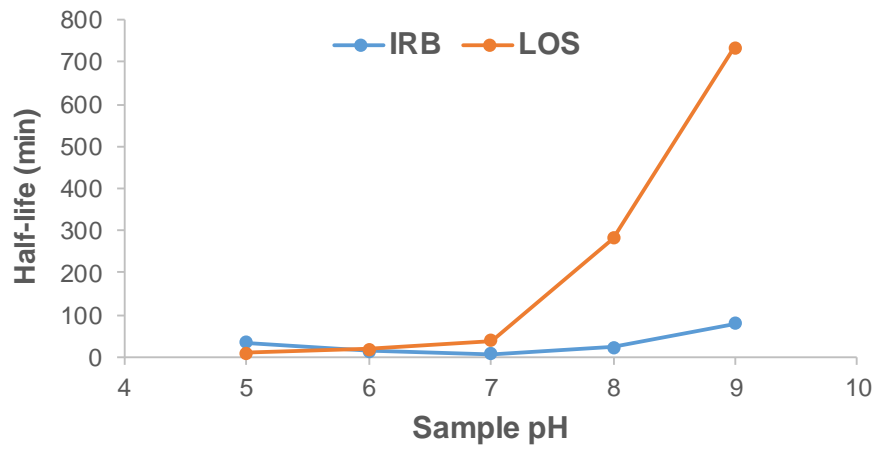


Fig. 1

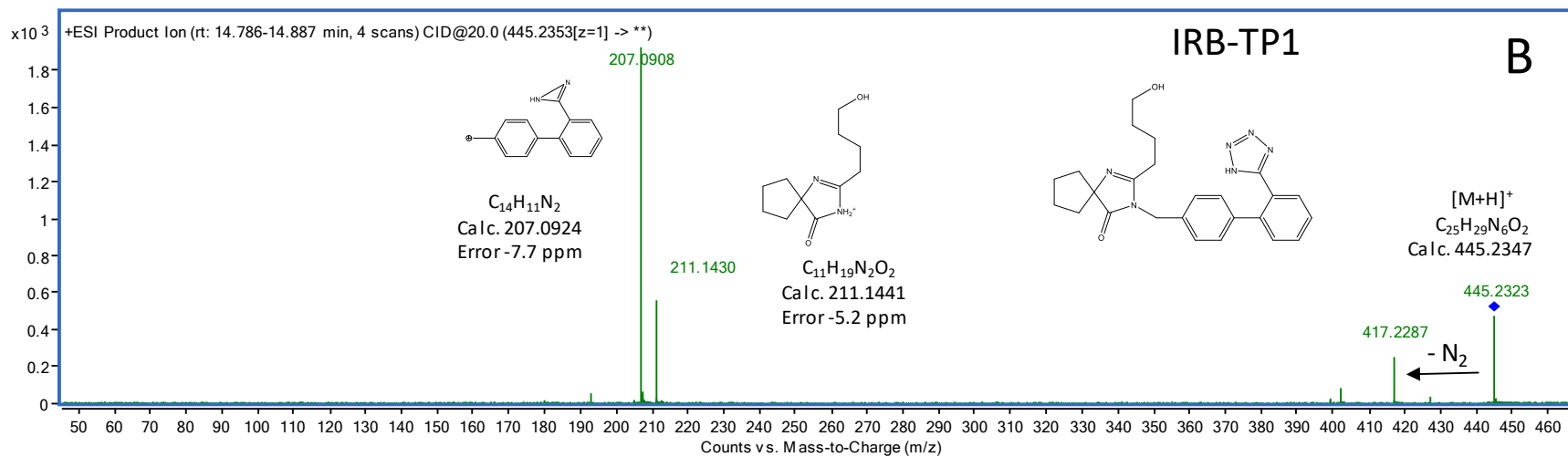
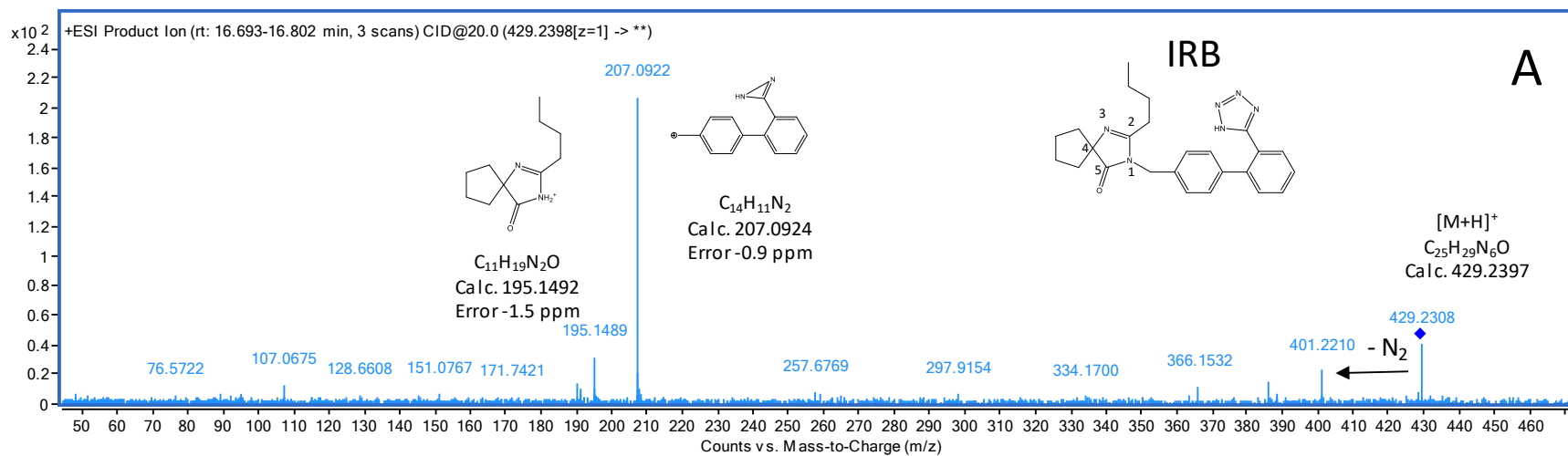


Fig. 2.

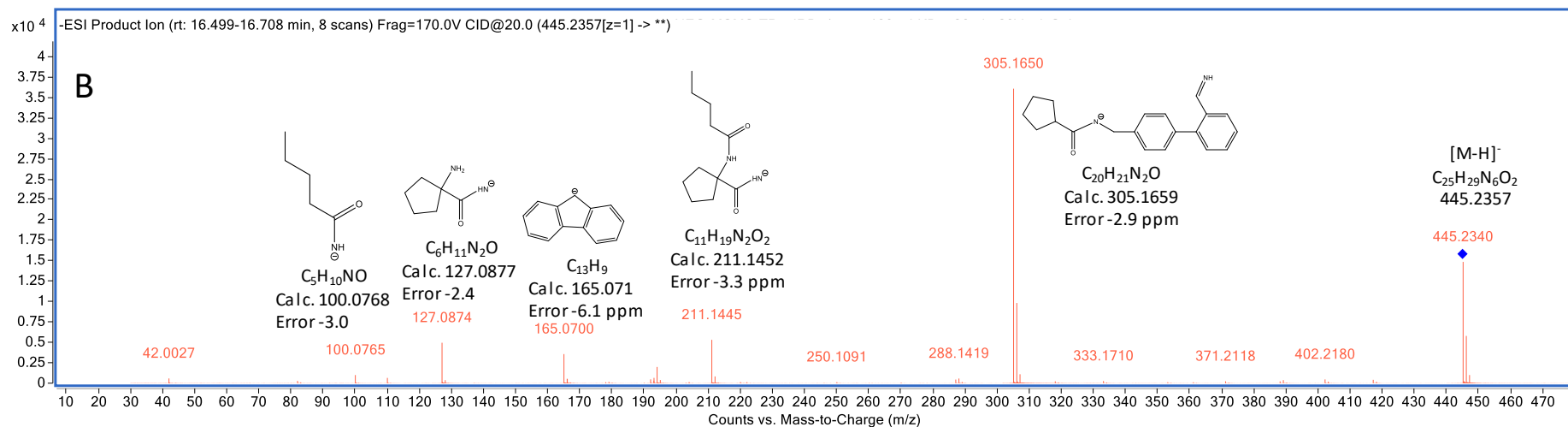
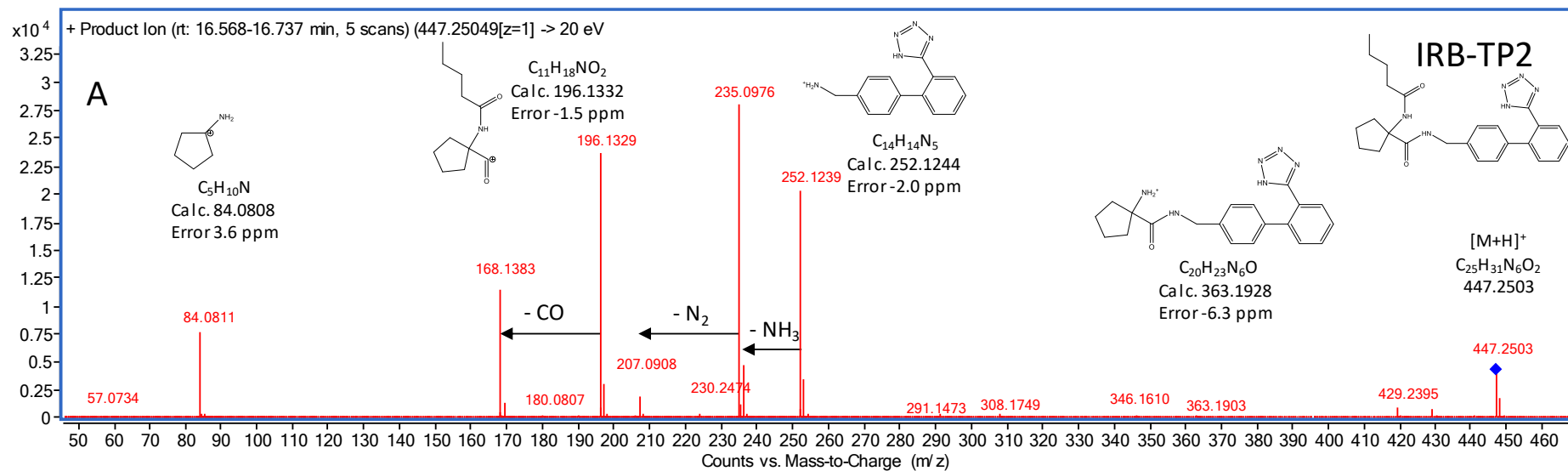


Fig. 3.

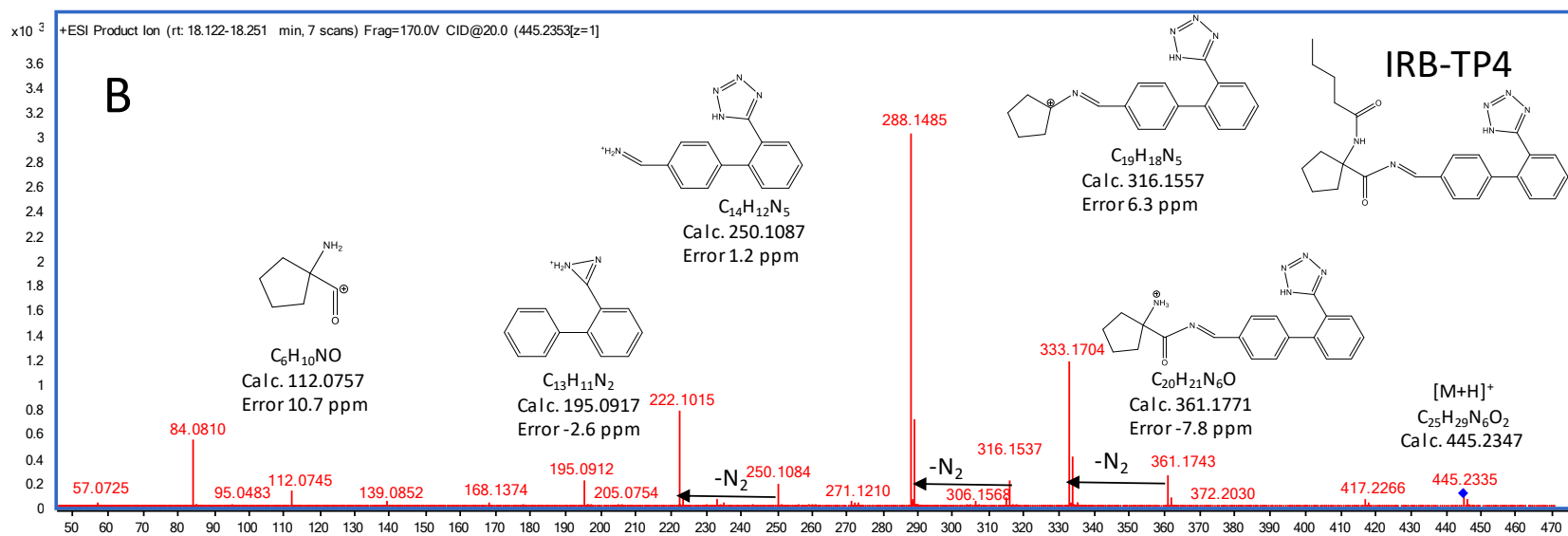
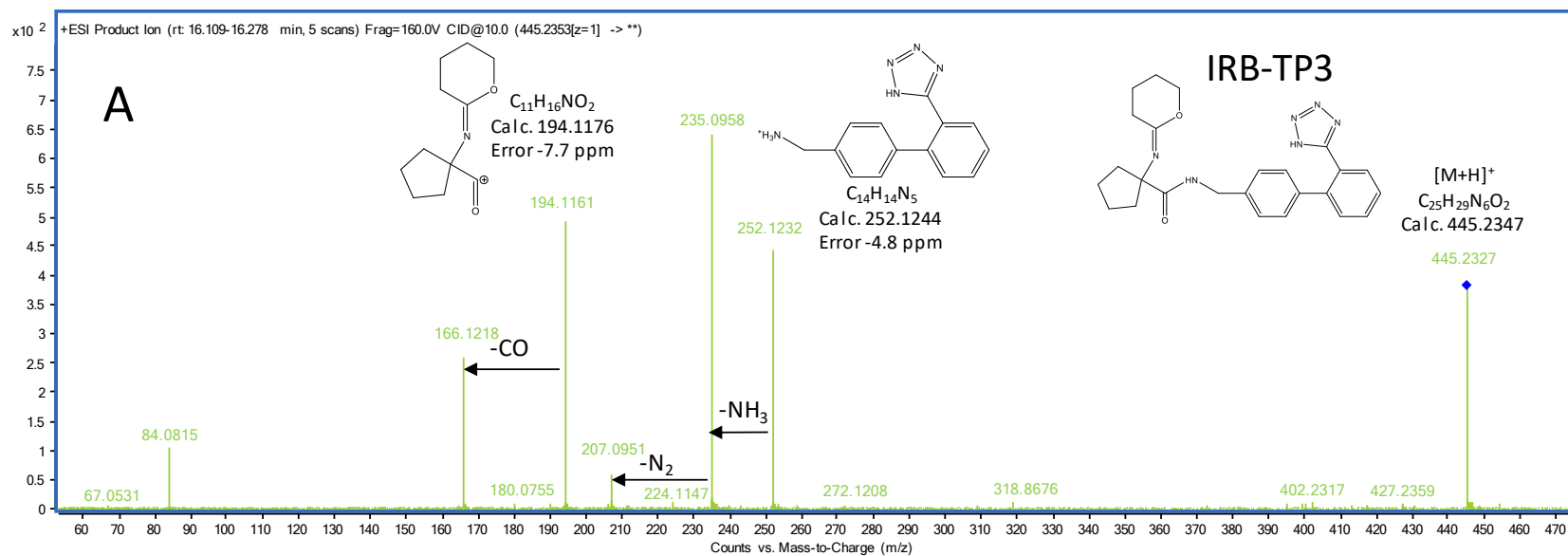


Fig. 4.

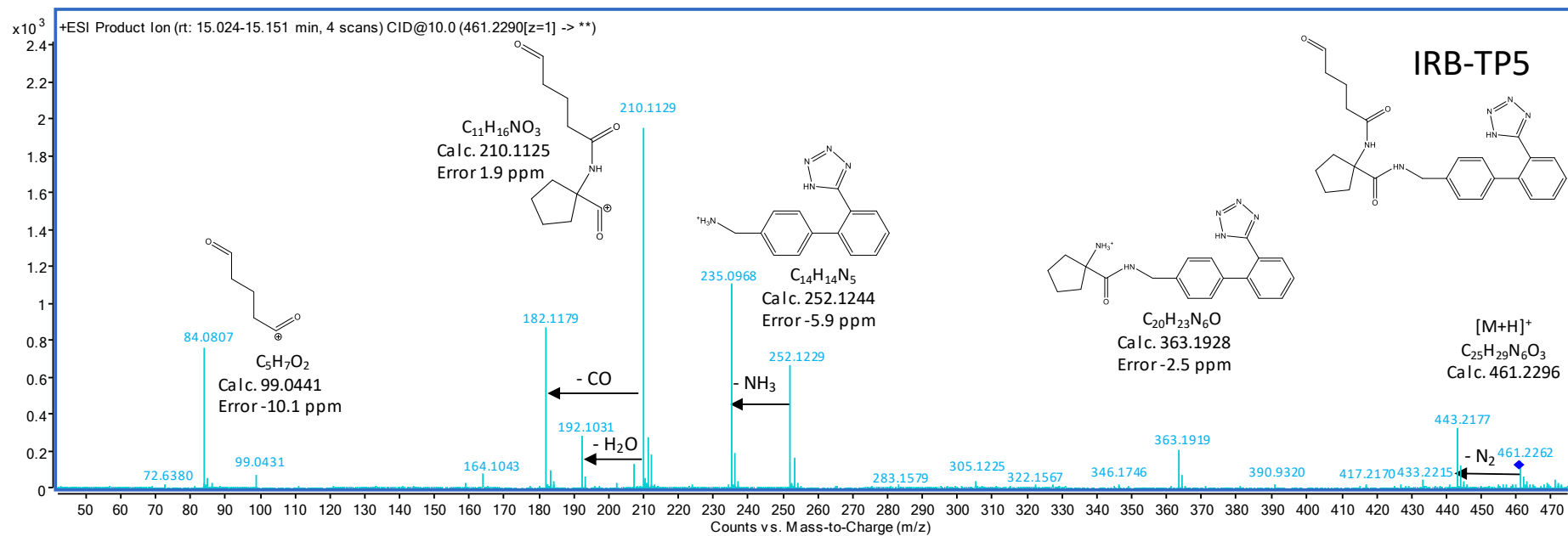


Fig.5.

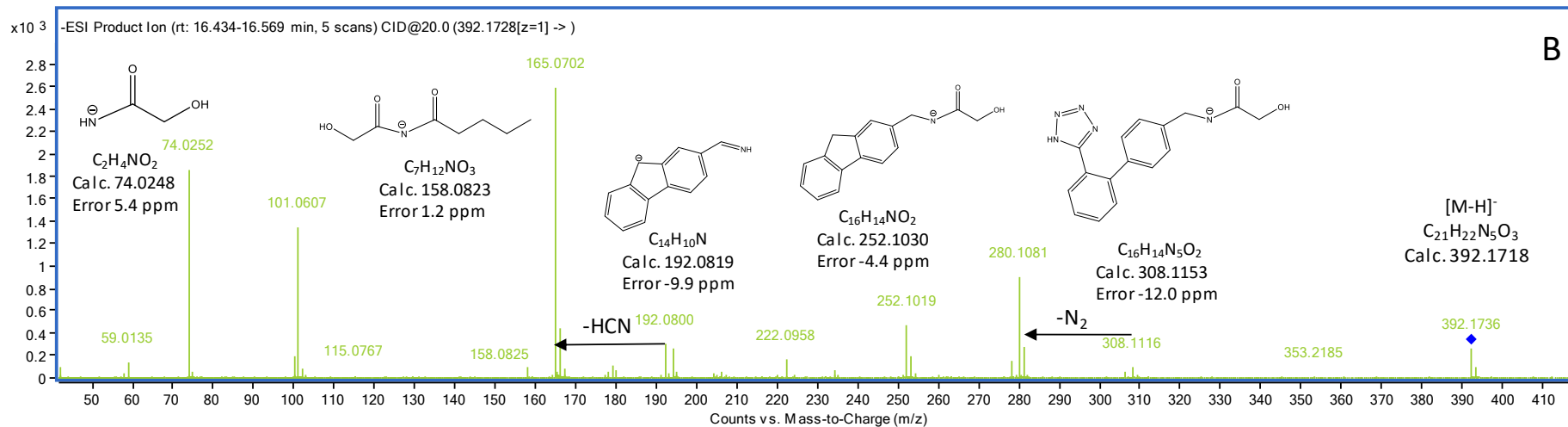
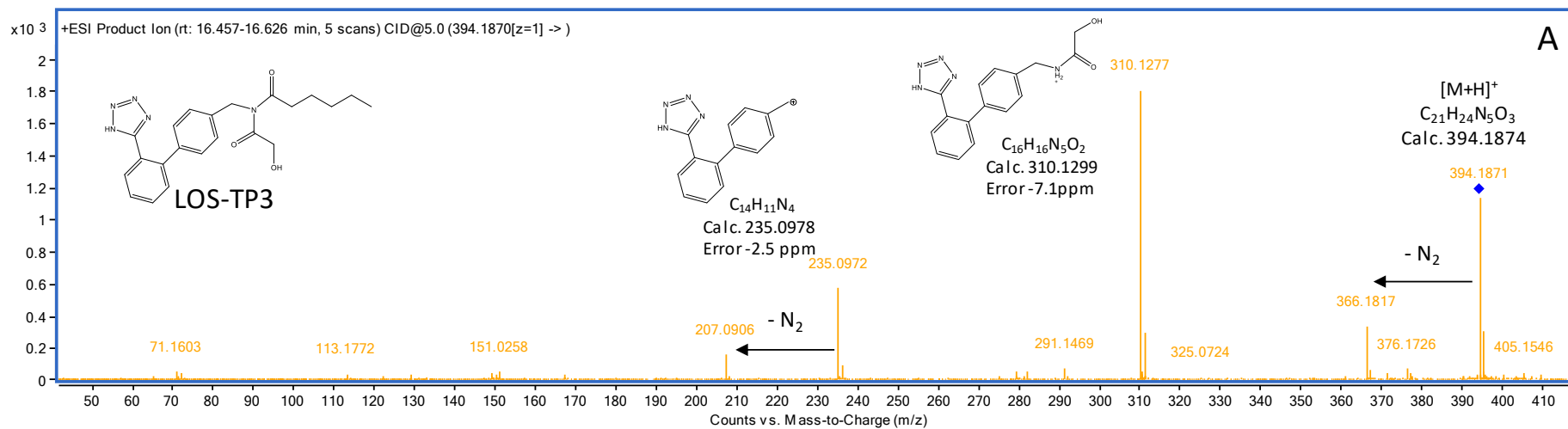


Fig. 6.

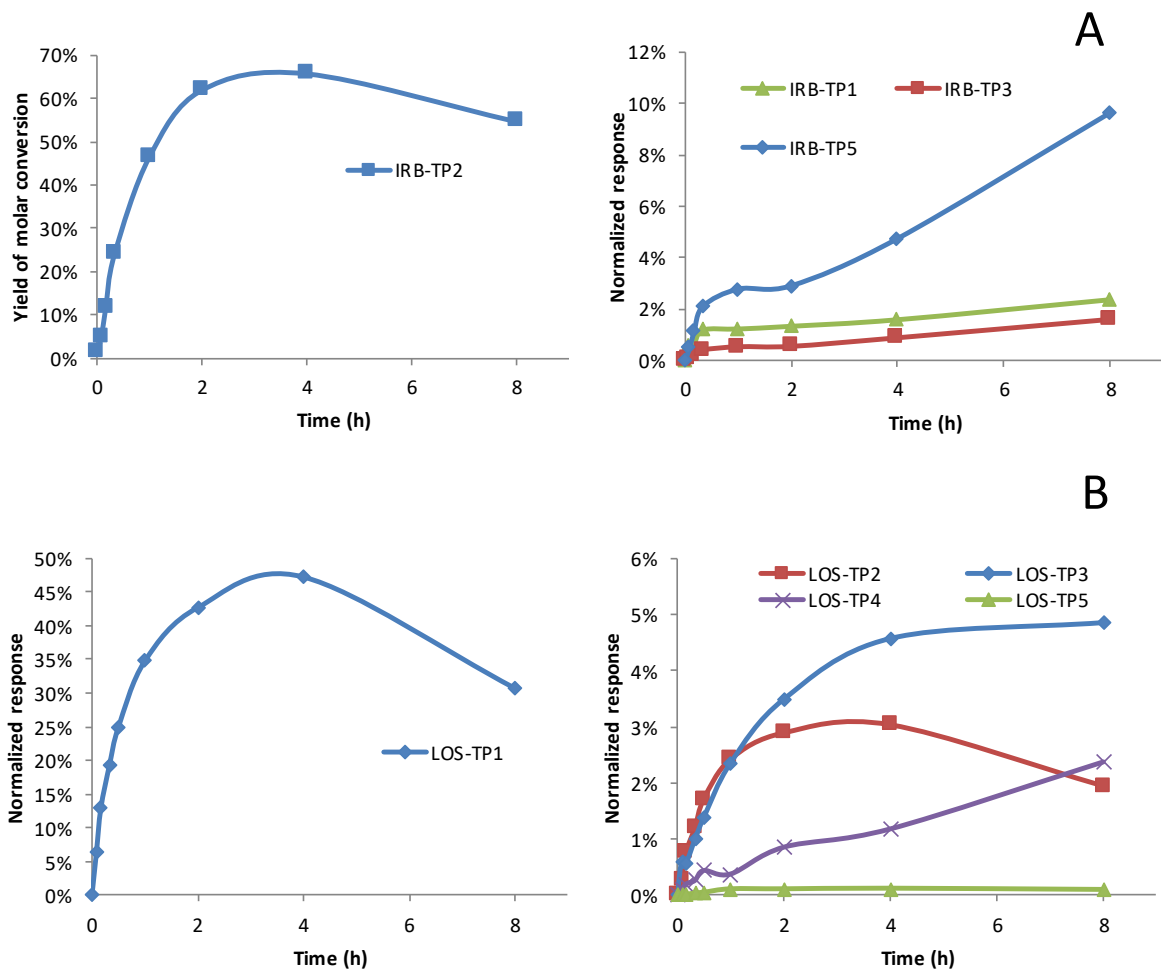


Fig. 7.

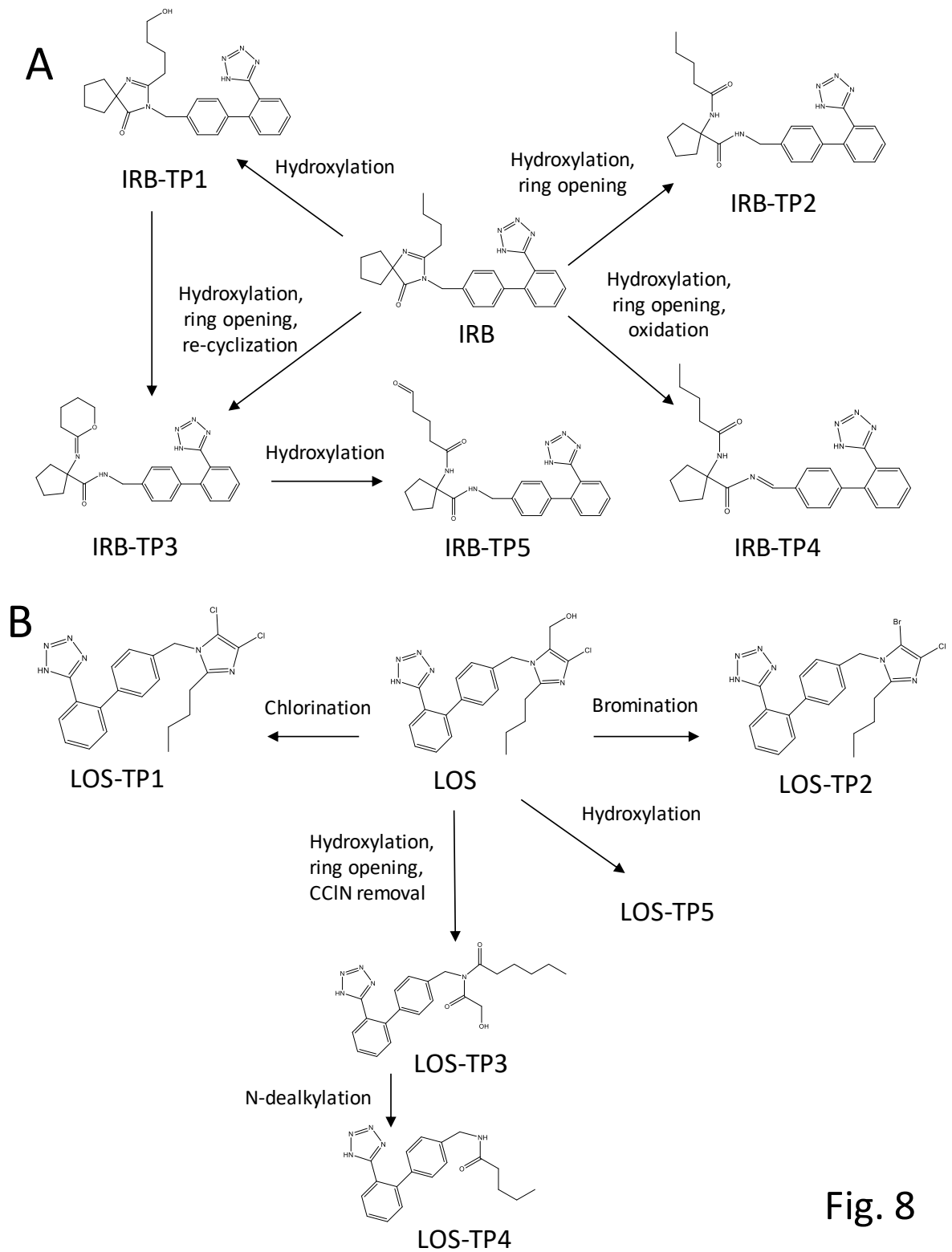


Fig. 8

Supplementary information to manuscript:

**Free chlorine reactions of angiotensin II receptor antagonists: kinetics study,
transformation products elucidation and in-silico ecotoxicity assessment**

I. Carpinteiro, G. Castro, I. Rodríguez*, R. Cela

Department of Analytical Chemistry, Nutrition and Food Sciences. Institute for
Research and Food Analysis (IIAA). Universidade of Santiago de Compostela, 15782
Santiago de Compostela, Spain.

*Corresponding author
e-mail: isaac.rodriquez@usc.es
Tel. 0034881814387

Table S1. Half-life ($t_{1/2}$, min) values, determination coefficients (R^2) for natural logarithmic plots of normalized responses (peak area divided by the peak area of the parent drug at zero time) versus reaction time, and second-order reaction rate constants (k , $M^{-1} \text{ min}^{-1}$) for IRB and LOS in ultrapure water solutions containing 10 mg L^{-1} ($1.41 \times 10^{-4} \text{ M}$) of free chlorine.

Compound	pH	$t_{1/2} \pm \text{SD}$ (min)	R^2	k ($M^{-1} \text{ min}^{-1}$)
IRB	5	35 ± 1	0.992	149 ± 5
	6	14 ± 1	0.990	345 ± 32
	7	6.2 ± 0.2	0.994	836 ± 24
	8	21.9 ± 0.5	0.997	236 ± 5
	9	79 ± 2	0.997	65 ± 2
LOS	5	9.4 ± 0.1	0.999	549 ± 8
	6	18.3 ± 0.6	0.997	282 ± 9
	7	39.5 ± 0.8	0.998	131 ± 3
	8	281 ± 7	0.997	18.4 ± 0.5
	9	734 ± 11	0.999	7.0 ± 0.1

Table S2. Ecotoxicological estimated data for acute and chronic exposure to IRB, LOS and their TPs. Predicted values obtained using the ECOSAR software. Chemical families employed in the QSAR predictions were amides (IRB and its TPs) and diazoles (LOS and its TPs).

Compound	Acute toxicity (mg L ⁻¹)			Chronic toxicity (mg L ⁻¹)		
	Fish LC ₅₀ (96 h)	Daphnid LC ₅₀ (48 h)	Algae EC ₅₀ (96 h)	Fish	Daphnid	Algae
IRB	0.32	0.19	0.13	0.02	0.1	0.35
IRB TP1	10.64	8.44	2.11	0.25	2.3	2.45
IRB TP2	38.77	34.18	5.97	0.67	7.19	5.08
IRB TP3	1.89	1.29	0.54	0.07	0.50	0.96
IRB TP4	21.37	17.87	3.7	0.43	4.25	3.64
IRB TP5	70.59	69.72	37.36	15.19	0.67	12.88
LOS	0.23	1.69	0.24	0.04	0.03	0.14
LOS TP1	0.0068	0.196	0.047	0.0077	0.0034	0.03
LOS TP2	0.0043	0.154	0.04	0.0066	0.0027	0.027
LOS TP3	0.263	2.22	n.a.	0.038	0.241	n.a.
LOS TP4	0.00011	0.014	0.0061	0.011	0.00025	n.a.

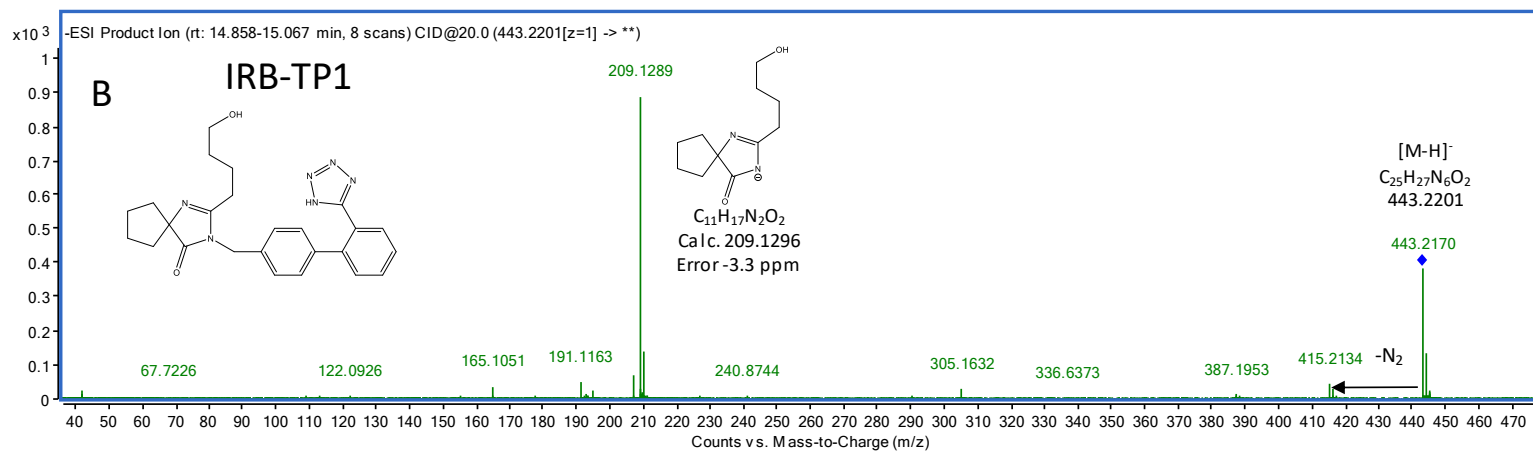
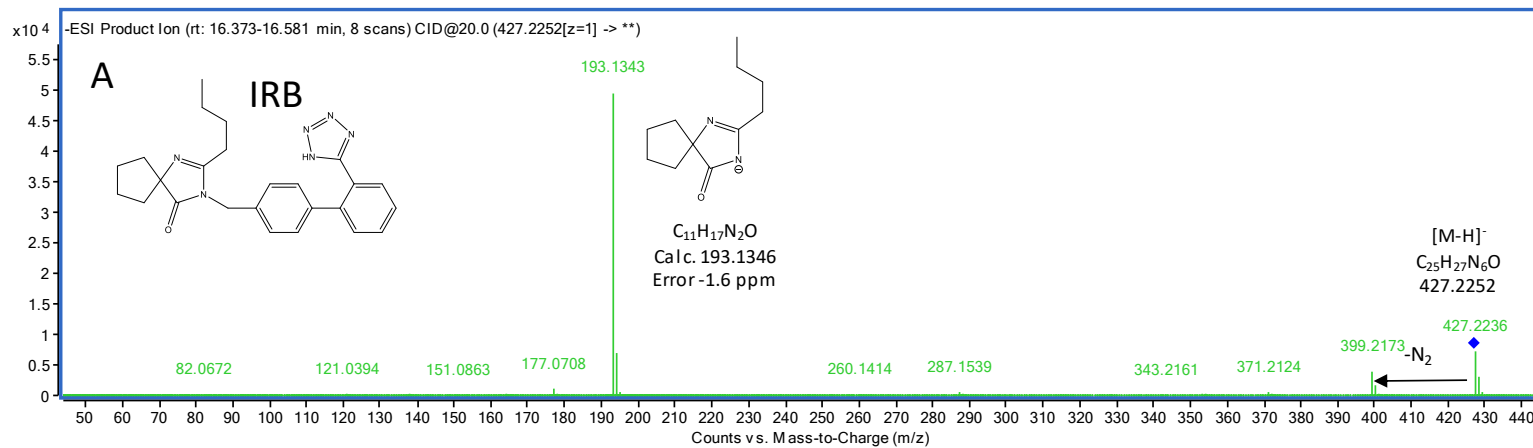


Fig. S1. ESI (-)-MS/MS spectra of IRB (A) and IRB-TP1 (B).

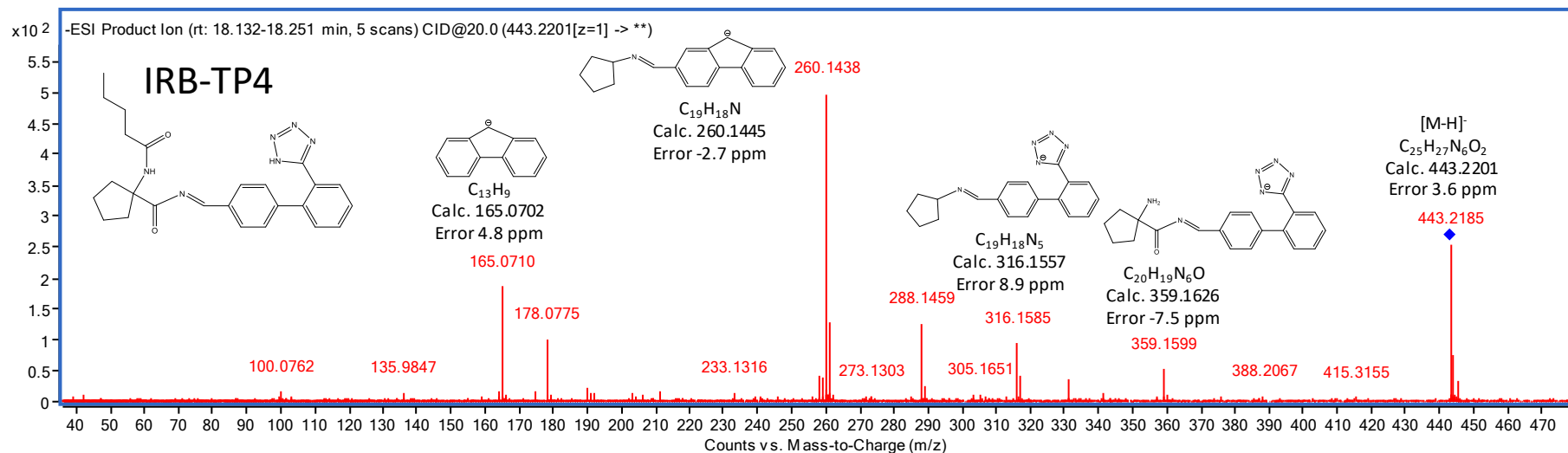


Fig. S2. Chemical structure (left) and ESI(-)-MS/MS spectrum, with fragments assignment, of compound IRB-TP4.

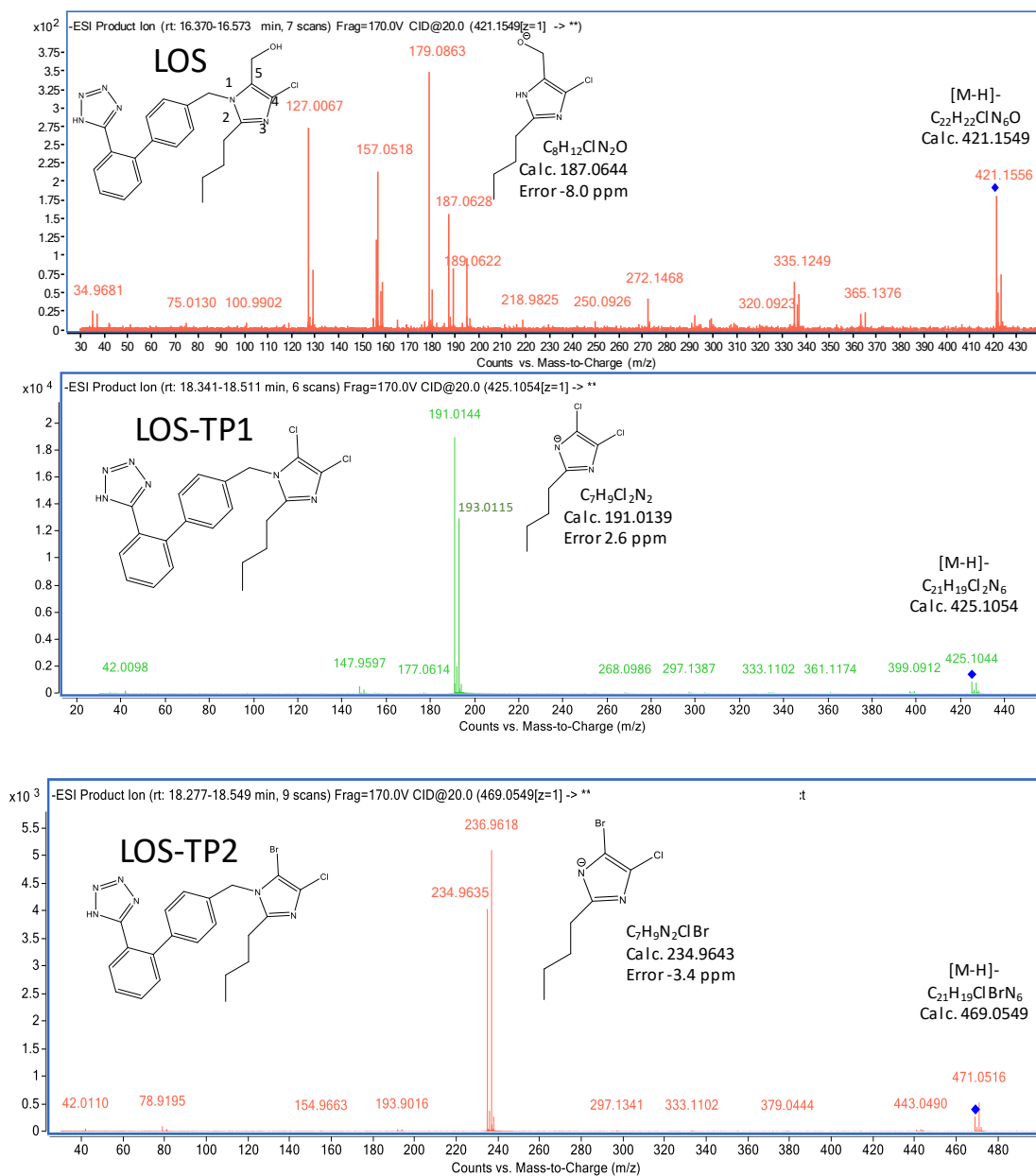


Fig. S3. Chemical structures and ESI(-)-MS/MS spectra of LOS, LOS-TP1 and LOS-TP2.

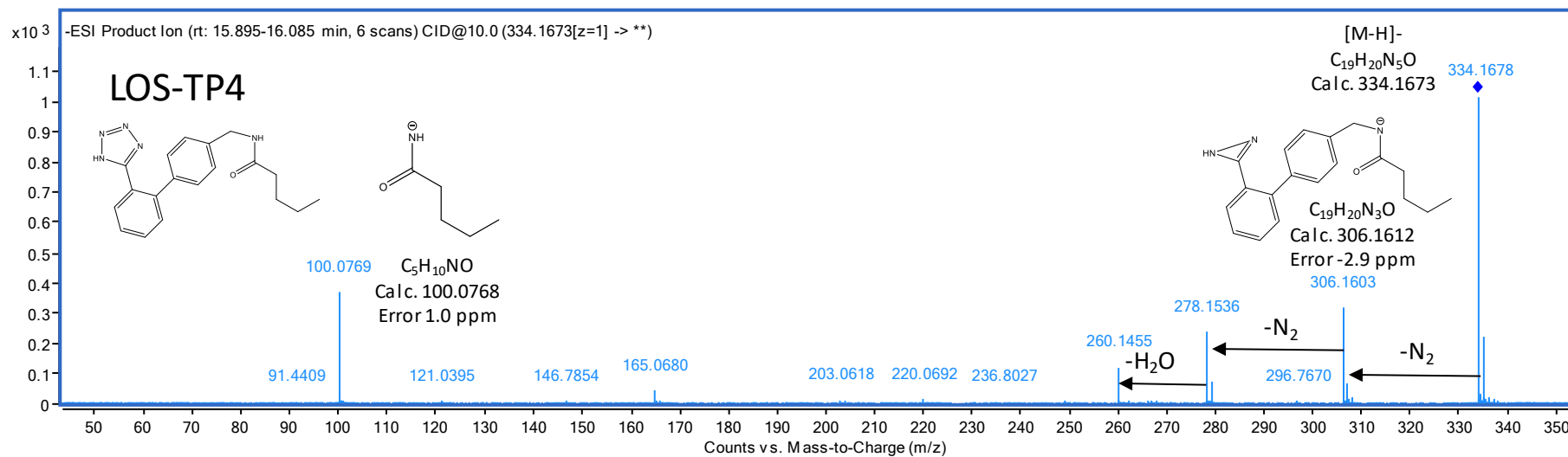


Fig. S4. ESI(-)-MS/MS spectrum for LOS-TP4.

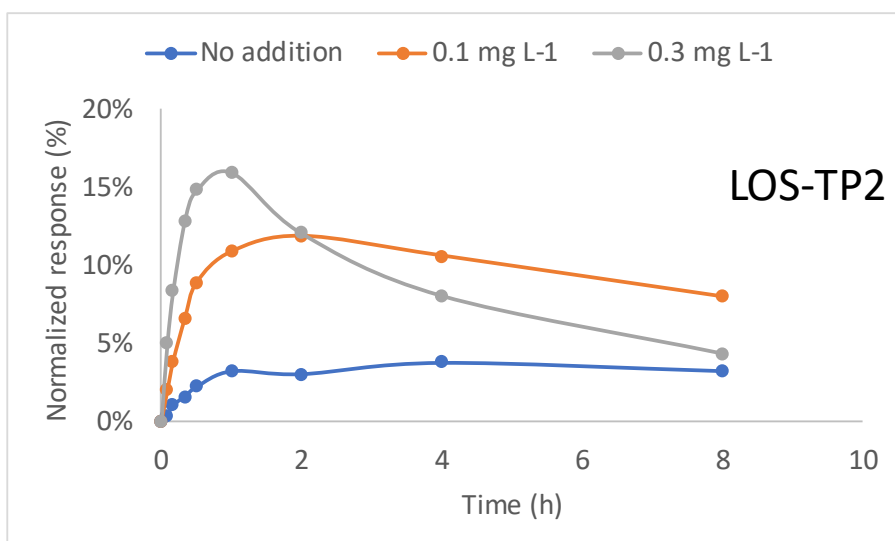
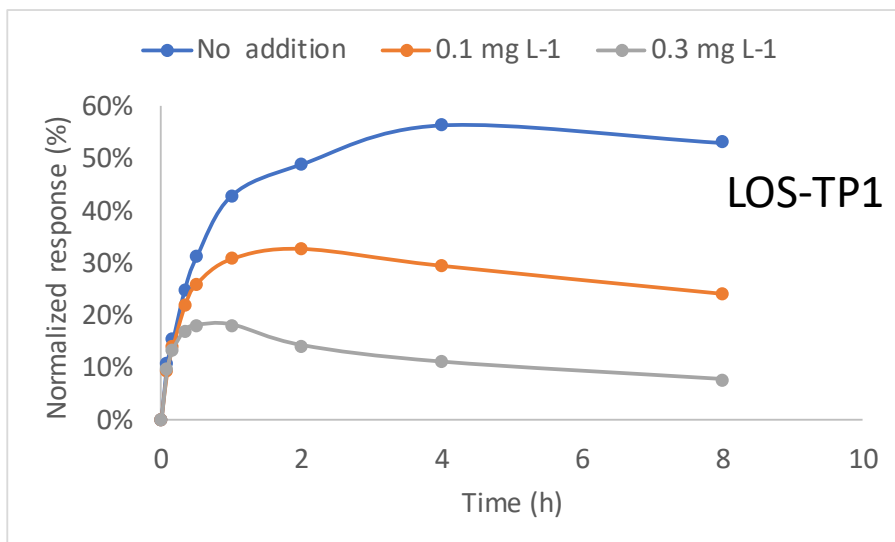


Fig. S5. Time-course of the dichloro (LOS-TP1) and the bromochloro (LOS-TP2) TPs of LOS in river water as function of the added bromide concentration. Data obtained at pH 7, using 10 mg L⁻¹ as the initial concentration of free chlorine. The unspiked water matrix contained 0.007 mg L⁻¹ of bromide.